PHYSICAL REVIEW B **88**, 161103(R) (2013)

Tunneling spectra simulation of interacting Majorana wires

Ronny Thomale,[1,2] Stephan Rachel,[3] and Peter Schmitteckert[4]

[1]*Institut de théorie des phénomènes physiques, École Polytechnique Fédérale de Lausanne (EPFL), CH-1015 Lausanne, France*

[2]*Institute for Theoretical Physics and Astrophysics, University of Würzburg, D-97074 Würzburg, Germany*

[3]*Institute for Theoretical Physics, TU Dresden, 01062 Dresden, Germany*

[4]*Institute for Nanotechnology, Karlsruhe Institute of Technology (KIT), 76344 Eggenstein-Leopoldshafen, Germany*

(Received 11 July 2013; published 7 October 2013)

Recent tunneling experiments on InSb hybrid superconductor-semiconductor devices have provided hope for a stabilization of Majorana edge modes in a spin-orbit quantum wire subject to a magnetic field and superconducting proximity effect. Connecting the experimental scenario with a microscopic description poses challenges of a different kind, such as accounting for the effect of interactions on the tunneling properties of the wire. We develop a density matrix renormalization group (DMRG) analysis of the tunneling spectra of interacting Majorana chains, which we explicate for the Kitaev chain model. Our DMRG approach allows us to calculate the spectral function down to zero frequency, where we analyze how the Majorana zero-bias peak is affected by interactions. For topological phase transitions between the topological and trivial superconducting phase in the Majorana wire, the bulk gap closure generically affects the proximity peaks and the Majorana peak.

DOI: 10.1103/PhysRevB.88.161103 PACS number(s): 71.10.Pm, 74.20.Rp, 74.45.+c, 74.78.Na

Introduction. The field of topological phases in correlated electron systems is witnessing enormous interest in contemporary condensed matter physics. A new stage has been set by the field of topological insulators and superconductors, which promoted the role of spin-orbit coupling from a quantitative relativistic correction to a substantial system parameter characterizing electronic quantum states of matter.[1,2] Aside from the fundamental significance on its own, this direction revitalized the search for Majorana bound states (MBS) as soon as Fu and Kane realized that topological insulators can induce MBS at the surface in proximity to a superconductor,[3] which could be detected through resonant Andreev tunneling at the surface.[4] Along with the challenging experimental effort to make these interfaces accessible,[5] Sau *et al.*[6] as well as Alicea[7] suggested alternative setups for such an effect via composite compounds of semiconductors and ferromagnetic insulators. Preceded by a milestone work of Kitaev,[8] this paved the way for theoretical proposals of one-dimensional versions of this scenario where a spin-orbit quantum wire is placed in proximity to a superconductor and subject to an applied magnetic field. There, Majorana modes are predicted to appear at the edge of the wire[9–12] and manifest themselves as a conductance peak.[4,13,14] The tunneling experiments by the Kouwenhoven group[15] along with subsequent independent accomplishments by other groups employing tunneling[16–20] and Josephson[21] measurements suggest that the spin-orbit quantum wires are an experimental scenario where MBS might be detectable: The InSb wires possess large spin orbit coupling, and appropriate contacts guarantee high transparency for electrons to induce superconducting (SC) gaps.[22] At the same time, the high Landé factor of InSb (Ref. 23) assures that one can still efficiently induce spin alignment in the wire by comparably low magnetic fields which do not significantly affect the SC proximity effect.

A first microscopic perspective on MBS emerged from the Pfaffian wave function in the context of paired Hall states[24,25] which was subsequently connected to the A phase of ^{3}He,[26] $p + ip$ superconductors,[27] and recently to optical lattice scenarios[28] as well as Majorana spin liquids.[29] MBS emerge as zero energy midgap states in the vortex solution of the Bogoliubov–de Gennes equation.[8,27,30–32] The MBS vortex state is protected through the emergent particle-hole symmetry of the superconductor and exhibits a vortex energy gap. Due to lack of phase space associated with the edges of the wire in the clean limit, the are no competing midgap states localized at the edge, suggesting that the MBS are protected by the full proximity gap $\Delta \sim 1K$.[15] Moreover, the tunability of several system parameters should make it feasible to observe the topological phase transition between a phase with and without MBS at the edge.

Various effects such as disorder, strength and direction of magnetic field, or temperature have been investigated for the Majorana wire.[33–46] This is an essential step to further understand experiments, as there are various alternative resonances induced by Josephson or Andreev bound states, Kondo physics, or disorder-imposed midgap states that could give rise to similar transport signals. Among all of these effects, the role of interactions is most complicated to address microscopically for a finite wire, as the Hamiltonian loses its bilinear form. As such, interactions cannot be easily treated for large system sizes unless a Luttinger liquid approximation is adopted where the proximity gap can only be included perturbatively, or interactions can only be considered in special scaling limits.[47–49] The mesoscopic limit $q,\omega \to 0$ suggests that the low energy treatment of tunneling experiments only depends on the existence of Majorana edge modes irrespective of the spectral properties in the bulk. This assumption, however, is invalid for any ac-type measurement at finite ω and for dI/dV_{SD} dc measurements at finite bias, where V_{SD} is the source-drain voltage.

In this Rapid Communication, we develop a density matrix renormalization group (DMRG) ansatz to study the role of interactions in Majorana wires by computing the full spectral function down to zero frequency. DMRG has been previously employed to obtain the doubly degenerate ground state of the Majorana wire.[50] The motivation to formulate a DMRG ansatz for the full spectral function is twofold. First, this allows to investigate the role of interactions on a microscopic level and connect its effects to the $dI/dV_{\rm SD}$ signal. In particular, the suspected Majorana zero-bias peak is centered around zero frequency, which would be hard to resolve in conventional time-resolved DMRG where an infinite time evolution would have to be performed. Second, we thus develop the platform to consider the interplay of effects such as disorder, temperature, and interactions in a most suited microscopic framework, which is likely to stimulate a subsequent quantitative analysis of experimental scenarios.

Model. We consider the effective description along the proposal by Kitaev[8] for a single open chain:

$$\mathcal{H} = \sum_{i=1}^{M-1}(-tc_i^\dagger c_{i+1} + \Delta c_i c_{i+1} + \text{H.c.}) - \mu \sum_{i=1}^{M} n_i + \sum_{i=1}^{M-1} V n_i n_{i+1}, \tag{1}$$

where $n_i = c_i^\dagger c_i$, M denotes the number of sites, t the nearest-neighbor hopping (set to unity in the following), Δ the proximity gap, μ the chemical potential, and V the nearest-neighbor Hubbard interaction. For $V=0$, the system can be studied analytically in a single-particle picture.[8] As a function of μ, a topological phase transition is driven between a bulk-gapped SC wire with ($|\mu| < 2t$) and without ($|\mu| \geqslant 2t$) one Majorana mode per edge which are still entangled, whereas correlations decay at the scale $\sim 1/\Delta$ in the bulk. The spectral signature of this is given by a ground state degeneracy for the two different parity sectors $P = (-1)^{\sum_i n_i}$ labeled even ($P=1$) and odd ($P=-1$). For the ground state in the even case, all electrons pair and avoid the proximity gap scale. For the odd case, the excess electron pays a Bogoliubov excitation energy $\sim\Delta$ in the trivial SC phase of the wire, while it can be located in the zero energy entangled state in the topological SC phase of the wire as provided by the Majorana edges. Accordingly, a single electron in transport takes advantage of the zero energy fermionic state formed by the two Majorana edges, yielding a shift in the quantized conductance and a zero-bias peak in the $dI/dV_{\rm SD}$ signal.[4,13,14] In particular, the energy location of the fermionic state energy formed by the Majorana edges is protected by particle-hole symmetry: As soon as the SC phase forms in the wire, the MBS does not evolve in energy and hence should give a zero-bias peak irrespective of modifications imposed on the wire which leave the specific SC phase intact, i.e., which do not close the bulk gap. From a different perspective of one-dimensional systems, the nontrivial phase of (1) can also be labeled topological[51] in the sense that the bulk gap forms without breaking continuous lattice symmetries, and yields fractionalized edge modes as compared to the constituent fermions which span the Hilbert space of the system. This is similar to the Haldane gap scenario of $S=1$ chains where the featureless bulk is gapped and the edges form $S=1/2$ degrees of freedom.[52]

The second line in (1) represents the most short-range interaction term between the fermions allowed by Pauli principle. While the proximity of the superconductor will be efficient in screening the long-range part of generic Coulomb interactions between the electrons, the short-range potential is less affected and needs to be considered. We treat finite size realizations of (1) up to $M=200$ for specific points, and compute the spectral function $A(\omega)$, i.e., the local single-particle density of states, which dictates the $dI/dV_{\rm SD}$ signal of a tunneling current I.

Method. The spectral function is obtained from the imaginary part of the retarded Greens function

$$\mathcal{G}^{\rm r}(z) = \mathcal{G}^{+}_{\hat{c}_x,\hat{c}_x^+} - \mathcal{G}^{-}_{\hat{c}_x^+,\hat{c}_x}, \tag{2}$$

$$\mathcal{G}^{\pm}_{\hat{A},\hat{B}}(z) = \langle\Psi_0|\hat{A}\,(E_0 - H \pm z)^{-1}\,\hat{B}|\Psi_0\rangle, \tag{3}$$

where $\hat{A}$ and $\hat{B}$ are placeholders for the operators of interest $(\hat{c}_{x_0},\hat{c}_{x_0}^+)$, $|\Psi_0\rangle$ is the ground state with energy E_0, x_0 denotes the position where the local density of states is evaluated, and $z=\omega+i\eta$ the complex frequency including the level broadening which has to be introduced to smear over finite size effects.[53] We evaluate the resolvent equations (3) by expanding

$$f_\pm(\mathcal{H}-E_0,z) = \frac{1}{E_0 - \mathcal{H} \pm z} \tag{4}$$

into Chebyshev orthogonal polynomials T_n,[54,55]

$$f_\pm(z,x) = 1/(\pm z - x) = \sum_{n=0}^{\infty} \alpha_n^\pm(z) T_n(x), \tag{5}$$

$$\alpha_\pm(z) = \frac{2/(1+\delta_{n,0})}{(\pm z)^{n+1}(1+\sqrt{z^2}\sqrt{z^2-1}/z^2)^n\sqrt{1-1/z^2}}. \tag{6}$$

In contrast to the standard kernel polynomial scheme,[56] we evaluate the expansion at a finite broadening η,[53,55] with the local density of states

$$A(\omega) = -\frac{1}{\pi}\lim_{\eta\to 0^+}\mathcal{G}^r_{\hat{c},\hat{c}^+}(\omega+i\eta). \tag{7}$$

The moments $T_n = \langle\Psi_0|T_n(E_0-H)|\Psi_0\rangle$ are obtained using the recurrence relations for the Chebyshev polynomials and all $|\zeta_n\rangle = T_n(E_0-H)|\Psi_0\rangle$ states are added to the density matrix to optimize for the basis at each DMRG step. We exploit the parity quantum number, and are typically using at least 1000 states per DMRG block. For calculating the moments for the Chebyshev expansion, we perform a first calculation for the first ten moments only. We then restart the DMRG to increase the number of moments in several restarts up to $n=800$. As for the single-particle limit $V=0$, we verified our results against a generalized Bogoliubov transformation.[57] We deconvolute the applied $\eta = 0.1$ (0.17) of the $M=96$ (48) site systems as described in Ref. 53.

V-μ phase diagram. Figure 1 displays the numerical phase diagram as obtained from our DMRG approach: As a function of V and μ, the system can reside in the trivial and topological SC phase, as well as in an (incommensurate) density wave state (I)DW for strong repulsive coupling. The topological SC phase is detected by the twofold degenerate ground states belonging to different parity sectors. In contrast, the two ground states of the (I)DW phase belong to the same parity sector, where a distinction between IDW and DW can be made by analyzing the homogeneity of local densities and entropy signatures. The four different gapped phases are separated from each other by critical lines. We observe a strong renormalization of μ_c

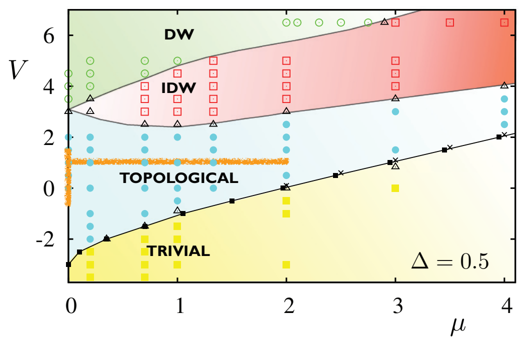

FIG. 1. (Color online) Phase diagram of (1) for $\Delta = 0.5$. Data points are obtained within DMRG for different system sizes: A trivial SC phase (yellow), the topological SC phase (light blue), an incommensurate density wave (IDW) (red), and a regular density wave (DW) phase (green) is found. Orange lines denote the parameter regions for Figs. 3 and 4.

separating the trivial and topological SC phase as a function of interaction strength. Our numerical phase diagram agrees quite well with the asymptotic analytic solution obtained by mapping the Kitaev chain to a Josephson junction array.[58] In particular, following the suggestion in Ref. 58, Josephson junction array scenarios establish a new arena where the Majorana wire interaction effects we investigate are relevant, as they can be tuned to strong interactions.

Δ dependence. We pick the phase space point $(V,\mu) = (1,0.5)$ located in the topological SC phase, and enhance the proximity scale Δ (Fig. 2). As soon as Δ is turned on, we find a clean Majorana zero-bias peak along with proximity peaks around $\omega = \pm\Delta$. Note that even though the system without an SC proximity term breaks particle-hole symmetry due to finite μ, the spectral function for the full model shows the expected emergent particle-hole symmetry for $|\omega| < \Delta$.

μ dependence. We fix V and investigate the behavior of the spectral function for increasing $\mu > 0$ as we trace through the topological SC phase along the horizontal orange line in Fig. 1. The holelike weight gets increasingly shifted to the electronlike regime, while the Majorana peak signal is robust independent of μ (Fig. 3).

V dependence. To show the specific evolution of the spectral function for varying interaction strengths, we trace a regime of V from weakly attractive to strongly repulsive in the topological SC regime (Fig. 4), as depicted by

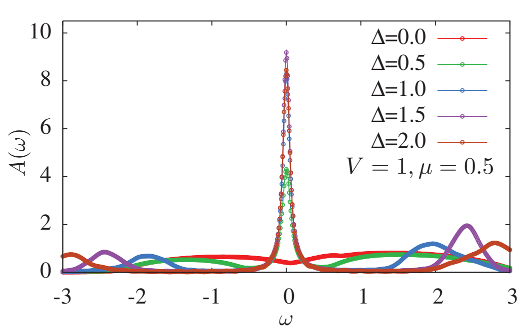

FIG. 2. (Color online) DMRG spectral functions $A(\omega)$ for different amplitudes Δ. ($M = 96$, $V = 1$, and $\mu = 0.5$.) The proximity peaks are asymmetric due to finite μ.

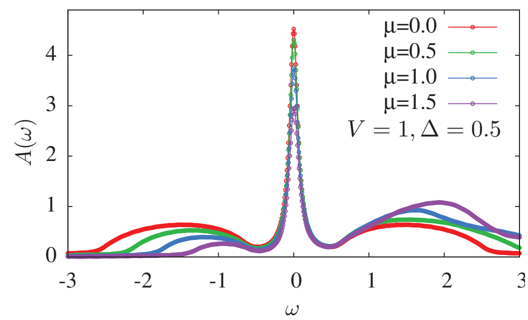

FIG. 3. (Color online) DMRG spectral functions $A(\omega)$ for different μ. ($M = 96$, $V = 1$, and $\Delta = 0.5$.)

the vertical orange line in Fig. 1. Weak attractive V sharpens the proximity peaks and enhances the Majorana zero-bias peak, along with the effective renormalization of the charge gap. The proximity peaks become broad due to repulsive V. Similarly, the zero-bias peak is sensitive to the interaction strength and quickly decreases in height as the interactions become repulsive. A major source of this effect is due to finite size effects such as the degeneracy splitting of the Majorana levels, which we checked to significantly vary as a function of interactions and system size. It relates to finite wave function overlap between the Majorana modes at the two ends.[34] The inset in Fig. 4 shows the FWHM divided by peak height of the zero-bias peak as a function of V, where a significant broadening is observed. It suggests that in the actual dI/dV_{SD} measurement, the zero-bias broadening is a combined effect of temperature and interactions.

Topological phase transition. An important feature of the topological SC phase with the Majorana zero-bias peak is the transport signature of phase transitions. Figure 4, if continued for higher V, would display the interaction-induced transition into a DW phase, where all previous main features such as the Majorana peak and the proximity peaks disappear. Figure 3, if continued to higher μ, would eventually illustrate the evolution of the transport signal into a trivial SC phase which also exists in the noninteracting case. There, a separate investigation of the Majorana peak and the proximity peaks, however, is

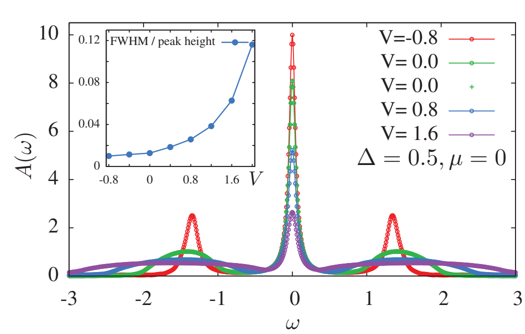

FIG. 4. (Color online) DMRG spectral functions $A(\omega)$ for various interaction strengths V. ($M = 96$, $\Delta = 0.5$, and $\mu = 0$.) Crosses for $V = 0$ denote the exact analytical solution, matching precisely with the according DMRG results. Moderate attractive V increases the Majorana peak height, while repulsive V suppresses the zero-bias peak. The Majorana peak broadens as illustrated in the inset displaying the FWHM divided by the peak height.

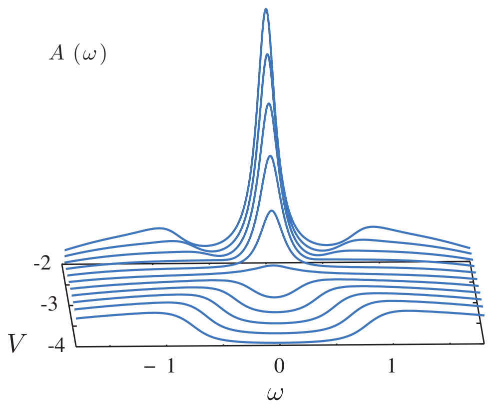

FIG. 5. (Color online) DMRG spectral functions $A(\omega)$ in the regime $V = -2, \ldots, -4$ in increments of 0.2. ($M = 48$, $\Delta = 0.5$, and $\mu = 0$.) The bulk-gap closure induces a joint collapse of the Majorana peak and the proximity gaps until the latter reopen in the trivial superconducting phase (Fig. 1).

quite hard to pursue because of the overpopulated electronlike Bogoliubov band. On fundamental grounds of characterizing topological phase transitions, at the transition between a trivial and a topological SC phase, the bulk gap must close. In turn, this implies that the Majorana peak cannot vanish without the proximity peaks being affected as well. To illustrate this aspect and also to choose a transition which might allow one to draw connections to the experimental setup where μ is held fixed,[15] we investigate the interaction-induced topological to trivial SC transition at $\mu = 0$ by varying V from -2 to -4 (Fig. 5). As we get closer to the transition, the Majorana peak shrinks along with a successive vanishing of the proximity gap until after the transition at $V_c \sim -3.0$, the proximity gap reopens without the Majorana peak. Since this is suitably kept in the DMRG spectral function, it suggests that it should generically be observed for a topological SC phase transition in the transport signal of Majorana wires. Note, however, that the leads and the Andreev reflectivity of the bulk-gap closing mode play a crucial role in connecting the tunneling density of states to a conductance measurement.

Summary and outlook. We have shown that the Chebyshev expansion method in DMRG allows us to obtain a detailed phase diagram of the Kitaev chain in the presence of interactions via spectral function calculations down to zero frequency. In the topological SC phase we find a clean Majorana zero-bias peak. Investigating the dependence of the spectral function on system parameters in the presence of interactions, we find that while μ changes the occupation of the holelike versus the electronlike Bogoliubov band, the Majorana zero-bias peak is hardly affected. The interactions modify the charge gap and as such, for one effect, renormalize μ_c separating the topologically trivial from the nontrivial SC phase in the wire. The interactions affect the height-width ratio of the Majorana peak. As the interactions reduce the bulk gap in the wire, the Majorana peak broadens and vanishes along with the proximity gap peaks. We have investigated differently tuned topological phase transitions and find that the bulk-gap closure manifests itself as a joint decay of the Majorana peak and the proximity gap. Our analysis establishes a starting point to endeavor the spinful Majorana wire models as well as to study joint effects of disorder, temperature, and interactions to establish a quantitative comparison with experimental signatures. Including explicit estimates for transmission curves, it will also be interesting to further analyze the possible renormalization of ac and dc conductance[49,59–62] in interacting Majorana wires.

Acknowledgments. We thank A. Akhmerov, B. Bauer, C. W. J. Beenakker, D. Goldhaber-Gordon, L. P. Kouwenhoven, R. Lutchyn, F. Pollmann, and D. Schuricht for discussions. R.T. is funded by DFG-SPP 1458 and ERC-StG-2013-336012. S.R. is funded by DFG-FOR 960 and DFG-SPP 1666.

[1] M. Z. Hasan and C. L. Kane, Rev. Mod. Phys. **82**, 3045 (2010).
[2] X.-L. Qi and S.-C. Zhang, Rev. Mod. Phys. **83**, 1057 (2011).
[3] L. Fu and C. L. Kane, Phys. Rev. Lett. **100**, 096407 (2008).
[4] K. T. Law, P. A. Lee, and T. K. Ng, Phys. Rev. Lett. **103**, 237001 (2009).
[5] J. R. Williams, A. J. Bestwick, P. Gallagher, S. S. Hong, Y. Cui, A. S. Bleich, J. G. Analytis, I. R. Fisher, and D. Goldhaber-Gordon, Phys. Rev. Lett. **109**, 056803 (2012).
[6] J. D. Sau, R. M. Lutchyn, S. Tewari, and S. Das Sarma, Phys. Rev. Lett. **104**, 040502 (2010).
[7] J. Alicea, Phys. Rev. B **81**, 125318 (2010).
[8] A. Y. Kitaev, Phys.-Usp. **44**, 131 (2001).
[9] R. M. Lutchyn, J. D. Sau, and S. Das Sarma, Phys. Rev. Lett. **105**, 077001 (2010).
[10] Y. Oreg, G. Refael, and F. von Oppen, Phys. Rev. Lett. **105**, 177002 (2010).
[11] C. W. J. Beenakker, Annu. Rev. Condens. Matter Phys. **4**, 113 (2013).
[12] J. Alicea, Rep. Prog. Phys. **75**, 076501 (2012).
[13] K. Flensberg, Phys. Rev. B **82**, 180516 (2010).
[14] M. Wimmer, A. R. Akmerov, J. P. Dahlhaus, and C. W. J. Beenakker, New J. Phys. **13**, 053016 (2011).
[15] V. Mourik, K. Zuo, S. M. Frolov, S. R. Plissard, E. P. A. M. Bakkers, and L. P. Kouwenhoven, Science **336**, 1003 (2012).
[16] H. A. Nilsson, P. Samuelsson, P. Caroff, and H. Q. Xu, Nano Lett. **12**, 228 (2012).
[17] M. T. Deng, C. L. Yu, G. Y. Huang, M. Larsson, P. Caroff, and H. Q. Xu, Nano Lett. **12**, 6414 (2012).
[18] A. Das, Y. Ronen, Y. Most, Y. Oreg, M. Heiblum, and H. Shtrikman, Nat. Phys. **8**, 887 (2012).
[19] A. D. K. Finck, D. J. Van Harlingen, P. K. Mohseni, K. Jung, and X. Li, Phys. Rev. Lett. **110**, 126406 (2013).
[20] E. J. H. Lee, X. Jiang, M. Houzet, R. Aguado, C. M. Lieber, and S. De Franceschi, arXiv:1302.2611.
[21] L. P. Rokhinson, X. Liu, and J. K. Furdyna, Nat. Phys. **8**, 795 (2012).
[22] Y.-J. Doh, J. A. van Dam, A. L. Roest, E. P. A. M. Bakkers, L. P. Kouwenhoven, and S. De Franceschi, Science **309**, 272 (2005).
[23] H. A. Nilsson, P. Caroff, C. Thelander, M. Larsson, J. B. Wagner, L. E. Wernersson, L. Samuelson, and H. Q. Xu, Nano Lett. **9**, 3151 (2009).

[24] M. Greiter, X. G. Wen, and F. Wilczek, Phys. Rev. Lett. **66**, 3205 (1991).
[25] G. Moore and N. Read, Nucl. Phys. B **360**, 362 (1991).
[26] G. E. Volovik, *The Universe in a Helium Droplet* (Clarendon, Oxford, 2003).
[27] N. Read and D. Green, Phys. Rev. B **61**, 10267 (2000).
[28] M. Sato, Y. Takahashi, and S. Fujimoto, Phys. Rev. Lett. **103**, 020401 (2009).
[29] M. Greiter and R. Thomale, Phys. Rev. Lett. **102**, 207203 (2009).
[30] N. B. Kopnin and M. M. Salomaa, Phys. Rev. B **44**, 9667 (1991).
[31] G. Volovik, JETP Lett. **70**, 609 (1999).
[32] D. A. Ivanov, Phys. Rev. Lett. **86**, 268 (2001).
[33] P. W. Brouwer, M. Duckheim, A. Romito, and F. von Oppen, Phys. Rev. Lett. **107**, 196804 (2011).
[34] A. M. Lobos, R. M. Lutchyn, and S. Das Sarma, Phys. Rev. Lett. **109**, 146403 (2012).
[35] S. Tewari, T. D. Stanescu, J. D. Sau, and S. Das Sarma, Phys. Rev. B **86**, 024504 (2012).
[36] C.-H. Lin, J. D. Sau, and S. Das Sarma, Phys. Rev. B **86**, 224511 (2012).
[37] T. D. Stanescu, S. Tewari, J. D. Sau, and S. Das Sarma, Phys. Rev. Lett. **109**, 266402 (2012).
[38] D. Bagrets and A. Altland, Phys. Rev. Lett. **109**, 227005 (2012).
[39] J. Liu, A. C. Potter, K. T. Law, and P. A. Lee, Phys. Rev. Lett. **109**, 267002 (2012).
[40] D. I. Pikulin, J. P. Dahlhaus, M. Wimmer, H. Schomerus, and C. W. J. Beenakker, New J. Phys. **14**, 125011 (2012).
[41] F. Pientka, G. Kells, A. Romito, P. W. Brouwer, and F. von Oppen, Phys. Rev. Lett. **109**, 227006 (2012).
[42] E. Sela, A. Altland, and A. Rosch, Phys. Rev. B **84**, 085114 (2011).
[43] S. Gangadharaiah, B. Braunecker, P. Simon, and D. Loss, Phys. Rev. Lett. **107**, 036801 (2011).
[44] A. Zazunov, A. L. Yeyati, and R. Egger, Phys. Rev. B **84**, 165440 (2011).
[45] E. Prada, P. San-Jose, and R. Aguado, Phys. Rev. B **86**, 180503 (2012).
[46] D. Rainis, L. Trifunovic, J. Klinovaja, and D. Loss, Phys. Rev. B **87**, 024515 (2013).
[47] R. M. Lutchyn and M. P. A. Fisher, Phys. Rev. B **84**, 214528 (2011).
[48] L. Fidkowski, J. Alicea, N. H. Lindner, R. M. Lutchyn, and M. P. A. Fisher, Phys. Rev. B **85**, 245121 (2012).
[49] R. Lutchyn and J. H. Skrabacz, Phys. Rev. B **88**, 024511 (2013).
[50] E. M. Stoudenmire, J. Alicea, O. A. Starykh, and M. P. A. Fisher, Phys. Rev. B **84**, 014503 (2011).
[51] A. M. Turner, F. Pollmann, and E. Berg, Phys. Rev. B **83**, 075102 (2011).
[52] F. D. M. Haldane, Phys. Rev. Lett. **50**, 1153 (1983).
[53] P. Schmitteckert, J. Phys.: Conf. Ser. **220**, 012022 (2010).
[54] A. Holzner, A. Weichselbaum, I. P. McCulloch, U. Schollwöck, and J. von Delft, Phys. Rev. B **83**, 195115 (2011).
[55] A. Branschädel and P. Schmitteckert (unpublished).
[56] A. Weiße, G. Wellein, A. Alvermann, and H. Fehske, Rev. Mod. Phys. **78**, 275 (2006).
[57] R. Korytar and P. Schmitteckert, arXiv:1307.1308.
[58] F. Hassler and D. Schuricht, New J. Phys. **14**, 125018 (2012).
[59] I. Safi and H. J. Schulz, Phys. Rev. B **52**, R17040 (1995).
[60] V. V. Ponomarenko, Phys. Rev. B **52**, R8666 (1995).
[61] D. L. Maslov and M. Stone, Phys. Rev. B **52**, R5539 (1995).
[62] R. Thomale and A. Seidel, Phys. Rev. B **83**, 115330 (2011).